

MOL # 44545

Human nocturnal frontal lobe epilepsy: pharmacogenomic profiles of pathogenic nAChR β -subunit mutations outside the ion channel pore

Jean-Charles Hoda, Wenli Gu, Marc Friedli, Hilary A. Phillips, Sonia Bertrand, Stylianos E. Antonarakis, David Goudie, Richard Roberts, Ingrid E Scheffer, Carla Marini, Jayesh Patel, Samuel F. Berkovic, John C. Mulley, Ortrud K. Steinlein and Daniel Bertrand
Department of Neuroscience, Medical Faculty, Geneva, Switzerland, J-CH, SB, DB
Department of Genetics, Medical Faculty, Geneva, Switzerland, MF, SA
Department of Cytogenetics and Molecular Genetics Centre for Medical Genetics, Women's and Children's Hospital, Adelaide, South Australia, HP, J-CM
Ninewells Hospital, Scotland, DG
Neurosciences Directorate, Tayside University Teaching Hospitals, Dundee, Scotland, RR
Department of Medicine (Neurology), University of Melbourne, Austin and Repatriation Medical Centre, Heidelberg, Melbourne, I-ES, CM, S-FB
Bristol Royal Hospital for Children, Department of Paediatric Neurology, Bristol, England, JP
Institute of Human Genetics, University Hospital, Ludwig Maximilians University Munich, Germany, GW, OKS

MOL # 44545

Running Title: Epilepsy and mutations in the nicotinic receptor

Correspondence to:

Daniel Bertrand, CH-1211 Geneva 4, Switzerland
Dep. of Neuroscience tel (41 22) 702 53 56
CMU
1, rue M. Servet fax (41 22) 702 54 02
e-mail: Daniel.Bertrand@medecine.unige.ch

Keywords: Nicotinic receptors, epilepsy, structure-function

Nb Pages:	30
Nb Figures:	7
Nb Tables:	2
Nb References:	38
Nb Words Abstract:	238
Nb Words Introduction:	423
Nb Words Discussion:	1485

Abbreviations: ACh, acetylcholine; nAChR, nicotinic acetylcholine receptor; ADNFLE, autosomal dominant nocturnal frontal lobe epilepsy.

MOL # 44545

Abstract

Certain mutations in specific parts of the neuronal nicotinic acetylcholine receptor (nAChR) subunit genes *CHRNA4*, *CHRNA2*, and probably *CHRNB2*, can cause autosomal dominant nocturnal frontal lobe epilepsy (ADNFLE). All but one of the known causative mutations are located in the second transmembrane region (TM2), which serves as the major ion pore-forming domain of the receptor. Functional characterization of these ADNFLE mutations have shown that while each mutant exhibits specific properties, they all confer a gain of function with increased sensitivity to acetylcholine. In this work we characterize the second and third ADNFLE associated mutations that are external to TM2 but affect different amino acid residues within the third transmembrane region (TM3). The two new *CHRNA2* mutations were identified in three families of Turkish Cypriot, Scottish and English origin. These TM3 mutations elicit the same gain of function pathomechanism as observed for the TM2 mutations with enhanced acetylcholine sensitivity, in spite of their unusual localization within the gene. Electrophysiological experiments including single channel measurements revealed that incorporation of these new mutant subunits do not affect the conductance of the ionic pore but rather increase the probability of opening. Determination of the sensitivity to nicotine for nAChRs carrying mutations in TM2 and TM3 showed clear differences in the direction and the extent to which the window current for nicotine sensitivity was shifted for individual mutations, indicating differences in pharmacogenomic properties that are not readily correlated with increased ACh affinity.

MOL # 44545

Introduction

Epilepsy is one of the most prevalent neurological disorders in the population and represents a life long impairment that is often difficult to treat. Recent progress has been made in understanding the molecular basis for a range of genetically based epilepsy syndromes (Heron et al., 2007). Autosomal dominant nocturnal frontal lobe epilepsy (ADNFLE) is one of the syndromes best-characterized at the molecular level (Mulley et al., 2003; Steinlein, 2002).

To date four mutations in *CHRNA4*, the gene encoding the $\alpha 4$ subunit of the neuronal nicotinic acetylcholine receptor (nAChR) have been identified ($\alpha 4$ -S248F, $\alpha 4$ -776ins3, $\alpha 4$ -S252L and $\alpha 4$ -T265I) (Hirose et al., 1999; Leniger et al., 2003; Steinlein et al., 1997; Steinlein et al., 1995). Similarly, three mutations have been reported for *CHRNA2*, the gene encoding the complementary $\beta 2$ subunit that participates in formation of the functional $\alpha 4\beta 2$ nAChR complex ($\beta 2$ -V287L, $\beta 2$ -V287M, $\beta 2$ -I312M) (Bertrand et al., 2005; De Fusco et al., 2000; Phillips et al., 2001). Recently, an additional mutation in the nAChR subunit gene *CHRNA2* ($\alpha 2$ -I279N) has been described in a family with an epilepsy phenotype closely resembling but probably not identical to the one seen in ADNFLE (Aridon et al., 2006).

In nAChR channels each subunit spans the membrane four times and the second transmembrane segment (TM2) contributes in a barrel like manner to the wall of the ionic pore (Bertrand et al., 1993). The first six mutations identified in ADNFLE patients were localized within or at the C-terminal end of TM2. While supporting the crucial contribution of this protein segment to receptor function, this observation suggested that only mutations in this domain could cause sufficient modification to the properties of the nAChRs to trigger ADNFLE seizures. This hypothesis was called into question when the first ADNFLE associated mutation located in TM3 of *CHRNA2* ($\beta 2$ -I312M) was described in 2005 (Bertrand et al., 2005). Now with two additional and previously undescribed *CHRNA2* TM3 mutations associated with ADNFLE, $\beta 2$ -L301V and $\beta 2$ -V308A, we set out to determine if they reiterate the observations made for $\beta 2$ -I312M, which suggested that TM3 mutations might be as important for the etiology of ADNFLE as the established TM2 mutations. Electrophysiological experiments including single channel

MOL # 44545

measurements revealed that incorporation of these new mutant subunits has effects on receptor properties that makes them readily distinguishable not only from wild type receptors but also show that the previously observed gain of function pathomechanism is common to both TM2 and TM3 mutations. Furthermore, nicotine sensitivity testing for different ADFLE mutations showed marked differences that are not readily correlated to the increased ACh affinity.

Methods

Mutation detection: We routinely amplified the transmembrane domains TM1, TM2 and TM3 of *CHRNA4* and *CHRNA2* by polymerase chain reaction (PCR) in ADFLE patients using the following primers: *CHRNA4* forward 5'-TCACCTATGCCTTCGTCATC-3', reverse 5'-TGGCACGATGTCCAGGAAGA-3', and *CHRNA2* forward 5'-TTCACACCTAGTGGTGAGTG-3', reverse 5'-TGGCTGCTGCATGAAGAGCA-3'. The PCR products were directly sequenced by Bigdye Terminator ready-reaction kit (PE Biosystems, Adelaide, Australia or Metabion, Planegg-Martinsried, Germany).

Mutation constructs: We introduced in the *CHRNA2* mutations for the $\beta 2$ subunit (Monteggia et al., 1995) using the PCR derived strategy described by Nelson and Long (1989). For $\beta 2$ -V287M and $\beta 2$ -L301V, the mutated fragment was ligated, after enzymatic digestion, at the unique NheI and PmlI restriction sites to the complementary wild type *CHRNA2* cDNA. The $\beta 2$ -V308A mutation was PCR-engineered from *CHRNA2* cDNA and cloned into the pRC/CMV vector (Invitrogen, Basel, Switzerland). Two overlapping PCR products, which contained the mutation, were obtained using $\beta 2$ mutf2-SP6 and $\beta 2$ mutr2-T7 primer couples. A second round of PCR was performed using a mix of the two previous PCR amplimers as a template with the flanking T7 and SP6 primers. The resulting full length *CHRNA2* cDNA with the mutation was then subcloned into the pTracer EF-A vector (Invitrogen, Basel, Switzerland) using EcoRV and XbaI restriction sites. All cDNA constructs were sequenced.

Oocyte expression: Oocytes were harvested from mature *Xenopus* females that were anaesthetized using tricaine and sacrificed according to animal ethic rules of Geneva canton, Switzerland. Ovaries were removed and stored at 4°C in physiological solution. Providing medium

MOL # 44545

was replaced at regular intervals, ovaries could be maintained for up to one month for oocyte preparation. Oocytes were isolated by mechanical and enzymatic digestion using type I collagenase (Sigma, Basel Switzerland) at 0.2 % in a medium deprived of calcium. Stage V and VI oocytes were manually selected using a binocular microscope and placed in BARTH medium that contained 88 mM NaCl, 1 mM KCl, 2.4 mM NaHCO₃, 10 mM HEPES, 0.82 mM MgSO₄ 7H₂O, 0.33 mM Ca(NO₃)₂·4H₂O, 0.41 mM CaCl₂·6H₂O, adjusted to pH 7.4 with NaOH and complemented with kanamycin (20 mg / ml), penicillin (100 U / ml) and streptomycin (100 U / ml). On the next day following dissociation, oocytes were injected in their nucleus with 2 ng of cDNA expression vector. For the expression of two cDNAs in homozygous mode (i.e. $\alpha 4$ and $\beta 2$, in a ratio 1:1) 1 ng of each cDNA was injected whereas for injection of three cDNAs in heterozygous mode (i.e. $\alpha 4$ and $\beta 2$ + $\beta 2$ V308A, in a ratio 1:0.5:0.5) 0.5 ng of $\beta 2$ and $\beta 2$ V308A cDNAs were injected together with 1 ng of the $\alpha 4$ cDNA. To minimize contamination each oocyte was kept in a separate well of a 96-well microtiter plate (NUNC) at 18°C. During incubation time oocytes were kept in BARTH solution.

Recording of nAChR properties: Two to three days after injection, oocytes were examined for current responses to ACh. Oocytes were impaled with two electrodes and their electrophysiological properties determined using a two-electrode voltage-clamp technique (GENECLAMP amplifier, Axon Instruments, Foster City, CA). Electrodes were made of borosilicate capillary glass pulled with a BB-CH-PC puller (Mecanex, Switzerland) and filled with filtered 3M KCl. Adequacy of the clamp was verified throughout the experiments by monitoring the voltage. Care was taken to use low impedance electrodes, always using the virtual ground, as specified by the manufacturer. These conditions allowed measurements of currents up to 30 μ A. During the experiments, oocytes were continuously superfused with OR2 (control medium) that contained 82.5 mM NaCl, 2.5 mM KCl, 2.5 mM CaCl₂, 1 mM MgCl₂, 5 mM HEPES, adjusted to pH 7.4 with NaOH. To mimic physiological conditions as closely as possible all experiments were carried out in a standard extracellular calcium concentration (2.5 mM). Solutions were gravity-fed at a flow rate of approximately 6 ml/min and controlled by computer-driven electromagnetic valves. Unless otherwise specified, the holding potential was -100 mV and experiments were performed at 18°C. To ensure the quality of agonist dose-response curves, concentrations were applied in

MOL # 44545

increasing order at time intervals of at least 2 minutes, which is sufficient to allow for full recovery of the ACh-evoked current. Assessment of oocyte conditions was made using standard 100 μ M ACh test pulses prior to and after dose-response curve determination. Only cells presenting no detectable rundown or cumulative desensitization were considered for analysis.

Transient transfection in HEK-293 and GH4-C1 cells: For patch-clamp recordings, human embryonic kidney HEK-293 cells were transfected with *CHRNA4* and *CHRN2* mutant cDNAs in the homozygous mode (ratio 1:1) together with pTracer cDNA (expressing a green fluorescent protein (GFP)). The FuGENE 6 transfection reagent (Roche Applied Science, Indianapolis, IN 46250) was used according to the manufacturer instructions. Transfection rate of $\alpha 4$ and $\beta 2$ mutants was indirectly monitored by the expression of the GFP. As a small percentage (<5%) of HEK-293 cells successfully transfected with $\alpha 4$ and $\beta 2$ -V308A cDNAs prevented single channel recordings, these cDNAs were also transfected in rat pituitary GH4-C1 cells using the same protocol where a higher yield of expression was observed. GH4-C1 cells were subsequently used for single channel recordings.

Single channel recordings: Single channels were measured in HEK-293 or GH4-C1 cells transiently transfected cells using the outside-out patch clamp configuration (Hamill et al., 1981). Briefly, the level of nAChRs expression was first evaluated using the whole-cell recording and brief ACh test pulses (30-100 μ M, 200 ms) as previously described (Buisson and Bertrand, 2001). As the $\alpha 4\beta 2$ nAChRs run down within a few minutes, attempts to pull outside-out patches were made only for cells displaying larger than average ACh-evoked currents. ACh was applied using the technique of liquid filament, as previously described (Buisson and Bertrand, 2001).

Curve fitting: ACh concentration-activation curves were best fitted by the sum of two empirical Hill equations, such as:

$$y = I_{\max} \left(\frac{a}{1 + (EC_{50H}/x)^{nH1}} + (1-a) / (1 + (EC_{50L}/x)^{nH2}) \right) \text{ (Equation (1))}$$

(Buisson and Bertrand, 2001; Covernton and Connolly, 2000). I_{\max} is the maximal current amplitude and x is the agonist concentration. EC_{50H} , $nH1$ and a are respectively the half-effective concentration, the Hill coefficient and the percentage of receptors in the high-affinity state whereas,

MOL # 44545

EC₅₀L and nH₂ correspond to the half-effective concentration and the Hill coefficient in the low-affinity state.

Concentration-inhibition curves were fitted using a single Hill equation in the form:

$$y = 1 / 1 + (x/IC_{50})^{nH} \text{ (Equation (2))}$$

where y is the current normalized to unity for the value recorded in control, x the concentration of the compound, IC₅₀ the half inhibition and nH the Hill coefficient.

Response decay times were fitted using a single exponential in the form $y = A \cdot \exp(-t/\tau) + B$ (Equation (3)) where A is the amplitude of the decaying current, t the time, τ the time constant in seconds and B the amplitude of the current at the plateau phase. Time zero for the exponential was set at the peak of the evoked current. Prior to fitting, curves were normalized to the maximal ACh-evoked current recorded at saturating concentration. For each cell, time courses were analyzed at 100, 50 and 25 % of the maximal response. Means and standard errors were obtained by pooling data measured in a series of oocytes for each of the mutants.

Statistics: Unless otherwise indicated all values are stated as mean \pm SEM. Statistical significance was evaluated using nonparametric Wilcoxon rank sum tests and a 5% desired level of significance (MATLAB, The Mathworks Inc.).

Results

Novel CHRN_{B2} TM3 mutations in ADFLE patients:

Family Hn is an Australian family of Turkish Cypriot origin. The 14 year-old male proband had nocturnal seizures starting at the age of 8 years. Attacks began with a breathless feeling or a feeling rising from the bottom half of his body, up to his chest and stiffening his body. His parents occasionally observed a grunting noise, eyes rolled up and pedaling movements of both legs. He remained aware, but was unable to talk. Attacks lasted 20 to 30 seconds in clusters of up to 10 per night. Seizures were not controlled by antiepileptic drug therapy. Interictal electroencephalography (EEG) showed frequent left fronto-central sharp transients. His 19 year-old brother had similar nocturnal episodes from 8 years of age that were documented with video-EEG and were consistent with frontal lobe seizures. Treatment with carbamazepine was effective and therapy was withdrawn in teenage. Their mother had similar nocturnal attacks from similar age. In teenage she

MOL # 44545

had clusters every night and was treated for a short time with diazepam. Nocturnal attacks persisted into adult life, but they were shorter, less frequent and she did not want treatment.

The three affected members of the Hn family had a TM3 mutation (c.901C>G) leading to a β 2-L301V substitution in *CHRNA2* (Fig. 1A). The β 2-L301 is conserved in other human nAChR subunit genes as well as in their orthologs (Fig. 1A+1B) with the exceptions of *CHRNA7*, *CHRNA9* and *CHRNA10*. Screening did not detect the β 2-L301V mutation in any other individual (100 anonymous blood donors, 150 patients suffering epilepsy other than ADNFLE or 80 sporadic and unrelated familial ADNFLE cases).

Family C is of Scottish origin. The 24 year-old Caucasian female proband had seizures from early childhood. Seizures comprise of sudden waking from sleep, a deep breath and then a sense of inability to breathe. Her arms and legs go rigid. Sometimes she grinds her teeth and cannot move for 15-20 seconds. She remains fully conscious throughout the attack. Video-EEG confirmed that these episodes were frontal lobe seizures. The seizures are well controlled with lamotrigine. Her mother has history of similar episodes, although these were much less frequent and severe. A maternal aunt and two cousins were similarly affected.

Mutation screening of the two available members of family C (the proband and her mother) revealed another TM3 mutation in *CHRNA2*, c.923T>C which gives rise to the β 2-V308A substitution (Fig. 1C). The β 2-V308 amino acid residue is fully conserved between species and among other nAChR subunits (Fig. 1D).

The β 2-V308A mutation was also found in the four affected members from an English three-generation family (family A138)(Fig. 1C). The 14 year-old female proband and her 16 year-old sister had nocturnal seizures starting at age 8 and 15 years, respectively. Seizure frequency in the proband was up to 5-10 attacks per night, while her sister only infrequently had seizures. In both the seizures responded well to carbamazepine. They had normal brain imaging (CT, MRT) and normal interictal EEG. Seizures are readily controlled with small doses of carbamazepine, and both girls perform well in school. The father started having nocturnal seizures in his early 20's and his epilepsy was treated but not sufficiently controlled with valproate. The paternal grandfather is also known to have nocturnal seizures starting at age 40 years but has never been treated. Seizures can occur every five minutes for up to 1-2 hours, and, like the other affected family

MOL # 44545

members, he has no recall of them. Both father and grandfather did well in their jobs and are not known to have any cognitive or psychiatric problems. Genotyping of three SNPs (single nucleotide polymorphisms) that are located in close vicinity to the mutation $\beta 2$ -V308A (rs2072659, rs2072660, rs2072661) demonstrated that all four affected members of the English family and the two patients from the Scottish family C share the same haplotype, but family sizes were too small to be conclusive about a possible relationship (or common founder) between both families (data not shown).

Functional properties of $\beta 2$ -L301V and $\beta 2$ -V308A:

Since all patients are heterozygous for the new TM3 mutations, functional experiments were carried out by co-expressing equal amounts of normal and mutant *CHRNA2* cDNAs together with wild type *CHRNA4* cDNA according to the method previously described (Moulard et al., 2001). Oocytes co-expressing the control and mutant subunits responded to ACh with robust currents comparable in magnitude to those recorded in cells expressing control subunits. The $\beta 2$ -L301V containing receptors were characterized by an increase in current amplitude at 1 mM ACh (173% of the value for control receptors recorded in sibling oocytes, Fig. 3A) and increased ACh sensitivity (Fig. 2A, filled squares, n=22; Table 1). In agreement with previous reports best fits were obtained with the sum of two empirical Hill equations (Equation (1)). Both the high and low affinity EC_{50} s decrease by a factor of about 1.5 (3.8 and 41.2 μ M for the $\beta 2$ -L301V mutant versus 5.8 and 63.9 μ M for the control; Fig 3B) but only the EC_{50H} was significantly different from the control. In parallel the fraction of the high affinity, represented by the parameter 'a', significantly increased by 2.2 fold (56% versus 25%; see Fig. 3B).

Similarly, when responses from cells expressing the $\beta 2$ -V308A mutant allele were compared to those of control a statistically significant difference in ACh sensitivity and current amplitude was observed. ACh-evoked currents were larger and decayed more slowly during the agonist application than the control (Fig. 2B, left panel). At 1 mM ACh currents were 39% larger than those measured in oocytes expressing control receptors (Fig. 3A). This increase in current amplitude was accompanied by an increase in ACh sensitivity (Fig. 2B; filled squares, n=10; Table 1). As for $\beta 2$ -L301V the mutation caused a reduction in both the high and low affinity EC_{50} s (1.6

MOL # 44545

and 37.4 μM versus 5.8 and 63.9 μM for the control; Fig. 3B). However, a significant difference was observed only for the high affinity component ($\text{EC}_{50\text{H}}$) of the mutant. Enhancement of the $\beta 2\text{-V308A}$ receptor function was further illustrated by the 2.1 fold increase of the fraction in the high affinity component (53% versus 25%).

Analysis of the response time course

While measurements of the mean current amplitude and agonist sensitivity provide a first estimation of a given receptor property, other parameters such as the response time course are also determinants of neurotransmission. For instance, it is well known that receptors presenting a faster rate of desensitization would impair synaptic transmission. Although desensitization is a complex mechanism a first approach in characterizing this property involves measuring the response decay time during the agonist exposure. To simulate natural conditions as close as possible all recordings were acquired in control medium. Neuronal nAChRs can flux a significant amount of calcium (Galzi et al., 1996; Sands and Barish, 1991; Séguéla et al., 1993), which could lead to the activation of calcium-activated currents, such as chloride currents that are endogenously expressed by oocytes. Minimization of chloride current contamination can be achieved either by reducing the extracellular concentration of calcium or by use of intracellular calcium chelating agents. However, these approaches present additional difficulties. Both extracellular and intracellular calcium concentrations have been shown to modify the nAChR responses. For instance, extracellular calcium ions have been shown to act as a powerful allosteric modulator (Galzi et al., 1996). Thus, divalent ion concentrations should be kept within their physiological range.

To characterize ACh-evoked responses in the control and mutant receptors, the experimental strategy was to first determine their dose-response profiles and then record the currents at ACh concentrations that evoked 25, 50 and 100% of the maximal responses for each receptor type. Recordings obtained from different cells in response to a 5s ACh application were normalized to the maximal current and the decay time was fitted to a single exponential equation (see methods; Equation (3)). A plot of the average time course is shown in Fig. 4A-D and illustrates the properties of control, $\beta 2\text{-L301V}$, and $\beta 2\text{-V308A}$ mutants. The best fits for the three ACh conditions and the four constructs are summarized in Table 2. These data clearly reveal the

MOL # 44545

contribution of the mutations to the response time course. In addition a slowing down of the response decay time was observed for the maximal ACh-evoked currents in the $\beta 2$ mutants compared to controls. This effect is best revealed when one compares the τ values for current decay as in Fig. 4E ($\beta 2$ -L301V, circles $n=9$ and $\beta 2$ -V308A triangles, $n=12$). The four-fold increase in the τ values for the $\beta 2$ subunit mutations was significant versus the control. Additionally, significant differences were detected in the amplitude of the plateau phase with up to a doubling of its value for the $\beta 2$ -L301V mutant.

To evaluate the possible contribution of chloride contamination the same experiments were repeated following incubation with the calcium chelating agent BAPTA-AM (100 μ M, overnight). Measurements of the response time course determined in oocytes loaded with BAPTA-AM are shown in Figure 4E-G and time constant obtained by curve fitting procedures similar to those previously described are summarized in panel H. These data indicate that no significant modification of the response decay time can be observed in presence of the BAPTA chelating agent and suggest a possible contribution of the chloride channels in the difference of time course observed in control conditions. These results are summarized in Table 2.

As oocyte perfusion yields limited time resolution, additional determination of the desensitization was examined in mammalian cells transfected with the control and mutated receptors. Results obtained using whole cell recordings and a fast drug application system with a piezoelectric driven liquid filament are summarized in Figure 5A. Electrodes were filled with EGTA (5 mM) containing medium, which buffers the intracellular calcium concentration and prevents contamination by calcium-activated currents. Results obtained in these experiments indicate no statistically significant differences in the time constant between control and mutated receptors (Student's t-Test > 0.05).

Single channel conductance is not affected by the mutations:

The best way to discriminate the mechanisms underlying the larger current amplitude observed in the whole cell is to examine single channel conductance. For this purpose cells were transfected with either the control (CT- $\alpha 4\beta 2$), one of the two new TM3 mutations ($\beta 2$ -L301V, $\beta 2$ -V308A) or, for comparison, one of the TM2 mutations ($\beta 2$ -V287M). Two to four days following transfection cells were investigated in patch clamp using whole cell and outside-out patch

MOL # 44545

configurations. For all the constructs investigated, typical single channel recording activity was observed in cells expressing large ACh-evoked currents (> 200 pA). As shown in Fig. 5 (traces, top panels) current deflections recorded during the ACh-application display comparable amplitude between the control (CT- $\alpha 4\beta 2$) and the three mutants ($\beta 2$ -V287M, $\beta 2$ -L301V and $\beta 2$ -V308A). Main single channel conductance was 42 to 46 pS for controls and all mutants investigated ($n \geq 5$ different patches for each construct). A very fast rundown with suppression of single channel activity within a minute or two was observed in all recordings independently of the expressed construct. Whole cell currents were obtained in 66 % of 50 cells tested for CT- $\alpha 4\beta 2$, 28.6 % of 140 cells tested for $\alpha 4\beta 2$ L301V and 15.8 % of 278 cells tested for $\alpha 4\beta 2$ V308A. Outside out patches were successfully obtained in 10% of CT- $\alpha 4\beta 2$, 3.6% of $\alpha 4\beta 2$ L301V and 1.8% of $\alpha 4\beta 2$ V308A expressing cells. Although the limited number of patches and fast rundown (less than 30s) prevents thorough analysis of single channel activity these data illustrate that the considered ADFLE mutations do not affect the single channel conductance and therefore that increase in current amplitude must be attributed to an increased probability of opening.

Altered sensitivity of mutant receptors to the nicotine:

As the ADFLE mutations in the $\alpha 4$ or $\beta 2$ subunits represent the first sets of non-synonymous variants reported in the human population, it is of value to examine if these mutations cause additional modification of the receptor properties. An obvious question is whether such mutation could correlate to smoking behavior and possibly alter nicotine sensitivity. Moreover, since nicotine was shown to provoke both activation and desensitization of the $\alpha 4\beta 2$ nAChR it is important to determine both parameters independently. Sensitivity to sustained nicotine exposure was tested using the protocol summarized in Fig.6 legend. A progressive desensitization of the ACh-evoked current was observed for controls and all the $\beta 2$ mutants (Fig. 6 A). Corresponding concentration-inhibition curves in Fig.6, panel B illustrate the difference of desensitization between the mutant receptors $\beta 2$ -L301V and $\beta 2$ -V287M in comparison to the control. The IC_{50} obtained for $\beta 2$ -V287M containing receptors was significantly lower than the IC_{50} calculated for controls ($IC_{50CT} = 63 \pm 21$ vs. $IC_{50\beta 2-V287M} = 9.2 \pm 1.3$, $p = 0.015$, Fig.6C) whereas the IC_{50} for $\beta 2$ -L301V was significantly higher ($IC_{50\beta 2-L301V} = 349 \pm 26$, $p = 0.005$, Fig.6C).

MOL # 44545

Nicotine concentration activation curves were determined over a broad range of concentrations by exposing cells to brief nicotine test pulses. Plot of the peak current evoked by nicotine as a function of the logarithm of the nicotine concentration yielded typical dose-response curve that are shown in Figure 7 (right traces in each four panels). A window current that is defined by the overlap between the desensitization and activation curves can be defined for the control and mutated receptors (indicated by gray areas). Notice a right shift of the window current for the $\alpha 4\beta 2$ -L301V and the $\alpha 4\beta 2$ -V308A whereas the $\alpha 4\beta 2$ -V287M displays a pronounced leftward shift. Altogether these data illustrate that mutation of a single amino acid in the $\beta 2$ subunit can cause a significant modification of the receptor sensitivity to nicotine confirming the pharmacogenomic relationship of ligand gated channels.

Discussion

Epilepsy is one of the most common neurological disorders, affecting at least 2% of the population at some time in life (Hauser et al., 1993). The finding of a naturally occurring mutation in *CHRNA4* associated with ADNFLE, a rare form of epilepsy, was the first demonstration that the genetic modification of a ligand-gated channel can cause seizures (Steinlein et al., 1995). This first observation was followed by a number of studies that have confirmed that functional disruption of ligand-gated channels can associated with epilepsy (Berkovic and Scheffer, 2001; Meisler et al., 2001)(Steinlein, 2008).

Localization of the mutations in the protein structure and receptor sensitivity

The first six reported ADNFLE mutations reported ($\alpha 4$ -S248F, $\alpha 4$ -259insL, $\alpha 4$ -S252L, $\alpha 4$ -T265I, $\beta 2$ -V287M or L) were all located within or juxtaposed to TM2. Therefore, it was first predicted that only mutations in this critical region would cause sufficient modification of the properties of the receptors to lead to ADNFLE. However, mutations in the neuromuscular junction nAChRs, which are responsible for certain congenital myasthenic syndromes, have been found in all five subunits of this class of receptor and are widely distributed along the protein sequence (Croxen et al., 2002; Croxen et al., 1997). Similarly, mutations of the structurally related glycine receptor associated with hyperekplexia have been found in different protein domains (Lewis et al., 1998; Rees et al., 2002). These observations are consistent with the role we now propose for

MOL # 44545

nAChR mutations located outside the TM2 domain, in the etiology of ADFLE (Bertrand et al., 2005).

Amino acid sequence comparison between various nAChR subunits demonstrates that the β 2-L301 and β 2-V308 residues are highly conserved. The position 301 corresponds to the break between the alpha helix and beta sheet structures of TM3 in the model proposed by Le Novère et al. (1999) (see Fig. 1C). An alternative hypothesis can be derived from the suggested structure of the *Torpedo marmorata* muscle receptor, resolved at 4 Å (Miyazawa et al., 2003). According to this high-resolution model the four transmembrane segments (TM1-TM4) of the muscle receptor span the membrane as alpha-helices. Moreover, these helices seem to protrude well beyond the extracellular and intracellular boundaries. This model would implicate strong interactions between TM2 and its adjacent TM1 or TM3 segments. Mutations in *CHRNA2*-TM3 could therefore alter the movement of TM2 by direct interaction in a comparable manner to that hypothesized for the TM3-V285I mutation in the α 1 muscle receptor subunit (Miyazawa et al., 2003). In this interpretation, the interaction between the non-moving TM3 and moving TM2 would be reinforced by longer amino acid side chains to reduce channel opening. Conversely, shorter amino acid side chains such as those observed in the TM3 ADFLE mutations could facilitate the motion of TM2 and promote opening of the gate that would be observable as an increase in the apparent ACh sensitivity.

ADNFLE mutations and the response kinetics

Analyses of the ACh-evoked responses (Fig. 2) shows that the responses of the receptors containing β 2-L301V and β 2-V308A had greater plateau values and decayed more slowly than controls. Analysis of the response decay time provides a first approximation of receptor desensitization kinetics. Desensitization is a complex mechanism that has been shown to depend upon multiple factors including the N-terminal structure of the receptor as well as phosphorylation of intracellular domains (Bohler et al., 2001; Fenster et al., 1999; Quick and Lester, 2002). Adequately described by a single exponential (see methods), the time constant τ exhibits a surprising relationship versus the ACh concentration for the *CHRNA2* mutants. The receptors containing β 2-L301V and β 2-V308A show indeed a higher plateau level and slower decay time at high ACh concentrations. Because the data were recorded in normal external calcium conditions it

MOL # 44545

could be claimed that responses are modified by the contamination by calcium activated chloride currents. Recordings obtained from oocytes in presence of a calcium-chelating agent (BAPTA) reveal no significant differences in the decaying time course, which suggests that the difference reported above might have been caused by the activation of chloride channels. Moreover, decay time measured using whole cell recordings in presence of EGTA in the intracellular medium show no difference in the response time course. Modifications in the kinetics of the response time course were reported for rat nAChRs that were engineered to harbor the ADNFLE mutations (Rodrigues-Pinguet et al., 2003). While for the rat nAChR, curve fitting was done only for one ACh concentration (about 40 μ M) and using the sum of two exponentials, it is interesting to note that for the control type nAChRs the fast decay time of human and rat receptors are similar. A faster decay time was also reported for the rat receptor into which the mutation corresponding to the human α 4-S252L was introduced (Matsushima et al., 2002). However, we observed that modification of the ACh response time course was not a common feature between the different mutations and can therefore not fully explain the triggering of ADNFLE seizures.

ADNFLE mutations do not modify single channel conductance

Changes in the mean current can be due either to higher surface expression of the receptors or to altered single channel properties. Studies performed on rat nAChRs in which ADNFLE mutations were introduced, showed that modifications of current amplitudes were not due to the differences in level of protein expression. Thus, it was concluded that these mutations do not detectably affect protein synthesis or receptor processing and insertion into the cell membrane (Rodrigues-Pinguet et al., 2003). In order to further understand the mechanisms linked to the changes described above, single channel measurements were performed. Recordings obtained in the outside-out configuration revealed that receptors containing mutations β 2-V287M, β 2-L301V and β 2-V308A display unitary conductance's (42-43 pS) similar to those of control receptors (46 pS). Although the very fast and profound run down of single channel activity prevented kinetic analysis, duration of openings seemed prolonged in the mutant receptors. These data suggest therefore that the increased ACh sensitivity and prolonged current duration induced by mutations in the TM3 domain of the β 2 subunit arise from modification of the allosteric properties of the receptor without changes in single channel conductance.

MOL # 44545

ADNFLE mutations change the response to nicotine

The physiological and behavioral effects of nicotine are primarily mediated by nAChRs and it was already reported that nicotine could act as an anti-epileptic agent by reducing seizures in ADNFLE patients harboring the $\alpha 4$ -776ins3 and $\alpha 4$ -S248F mutation (Brodtkorb and Picard, 2006). We therefore investigated the potential effects of nicotine on ADNFLE mutations located in either TM2 or TM3. The desensitization induced by nicotine was significantly more pronounced for the TM2 mutant $\beta 2$ -V287M than for the control, but was significantly decreased for the TM3 mutant $\beta 2$ -L301V in comparison to the control. However, depending on the range of nicotine concentrations investigated, it is also necessary to take the nicotine activation curve into account. Thus, it is even more physiologically relevant to examine the window current resulting from both desensitization and activation curve and reflecting the effective nicotinic current contribution among a range of concentrations (Fig.7). Interestingly, the window currents of the mutant $\beta 2$ -L301V and $\beta 2$ -V308A were slightly shifted to the right of the window current obtained for controls but it was leftward shifted in the case of the mutant $\beta 2$ -V287M (Fig. 7). These effects occurred independently from the increased ACh sensitivity common to all mutations. The mean physiological concentration of nicotine in smokers' brain varies from 0.06 to 0.4 μ M (Benowitz et al., 1989). In this range of concentrations, the total reduction (desensitization – activation contribution) of the ACh-evoked current due to nicotine was 20-50% for $\beta 2$ -L301V, 30-60% for $\beta 2$ -V308A, 45-70% for controls and 65-95% for $\beta 2$ -V287M. It is tempting to speculate that an ADNFLE patient carrying the mutation $\beta 2$ -V287M would better reduce their seizure susceptibility by smoking or other means of nicotine application than an ADNFLE patient carrying, for example, the mutation $\beta 2$ -L301V, assuming that inactivation by desensitization of the mutant receptors is responsible for the beneficial effect of nicotine. Although reduced seizure susceptibility by nicotine was only reported for carriers of CHRNA4 mutations, these differences provide new insights in the potential treatment of ADNFLE patients refractory to standard antiepileptic therapy.

Altogether the present data indicate that mutations in the TM3 domain of nAChR subunits such as CHRN2 are likely to be as important for the etiology of ADNFLE as previously shown for TM2 mutations. Mutations in TM3 increase the sensitivity to ACh, thus sharing the gain of function effect that has been proposed to be common to all previously described ADNFLE mutations. The

MOL # 44545

TM3 mutations do not increase the conductance of the ionic pore as demonstrated by single channel measurement suggesting a causal increase in the open probability of the channel. The various nicotine desensitization-activation profiles of different *CHRNA2* mutants investigated here revealed significant differences in the sensitivity to this natural alkaloid that are not correlated to the increased ACh affinity, emphasizing the pharmacogenomic link between single amino-acid changes and individual drug responses.

MOL # 44545

Acknowledgments

We are grateful to Drs R. Hogg and M. Lecchi for their helpful discussions and to C. Duret and D. Dias for their technical help. We thank Drs I. Favre and S. Weiland for their help in engineering the mutations β 2-V287M and β 2-L301V respectively.

MOL # 44545

References

- Aridon P, Marini C, Di Resta C, Brilli E, De Fusco M, Politi F, Parrini E, Manfredi I, Pisano T, Pruna D, Curia G, Cianchetti C, Pasqualetti M, Becchetti A, Guerrini R and Casari G (2006) Increased sensitivity of the neuronal nicotinic receptor alpha 2 subunit causes familial epilepsy with nocturnal wandering and ictal fear. *Am J Hum Genet* **79**:342-350.
- Benowitz NL, Porchet H and Jacob P, 3rd (1989) Nicotine dependence and tolerance in man: pharmacokinetic and pharmacodynamic investigations. *Prog Brain Res* **79**:279-287.
- Berkovic SF and Scheffer IE (2001) Genetics of the epilepsies. *Epilepsia* **42**:16-23.
- Bertrand D, Elmslie F, Hughes E, Trounce J, Sander T, Bertrand S and Steinlein OK (2005) The CHRNA2 mutation I312M is associated with epilepsy and distinct memory deficits. *Neurobiol Dis* **20**:799-804.
- Bertrand D, Galzi JL, Devillers-Thiery A, Bertrand S and Changeux JP (1993) Stratification of the channel domain in neurotransmitter receptors. *Curr Opin Cell Biol* **5**:688-693.
- Bertrand D, Picard F, Le Hellard S, Weiland S, Favre I, Phillips H, Bertrand S, Berkovic SF, Malafosse A and Mulley J (2002) How mutations in the nAChRs can cause the ADNFLE epilepsy. *Epilepsia* **43**:112-122.
- Bohler S, Gay S, Bertrand S, Corringer PJ, Edelstein SJ, Changeux JP and Bertrand D (2001) Desensitization of neuronal nicotinic acetylcholine receptors conferred by N-terminal segments of the beta 2 subunit. *Biochemistry* **40**:2066-2074.
- Brodtkorb E and Picard F (2006) Tobacco habits modulate autosomal dominant nocturnal frontal lobe epilepsy. *Epilepsy Behav* **9**:515-520.
- Buisson B and Bertrand D (2001) Chronic exposure to nicotine upregulates the human (alpha)4(beta)2 nicotinic acetylcholine receptor function. *J Neurosci* **21**:1819-1829.
- Covernton PJ and Connolly JG (2000) Multiple components in the agonist concentration-response relationships of neuronal nicotinic acetylcholine receptors [In Process Citation]. *J Neurosci Methods* **96**:63-70.
- Croxen R, Hatton C, Shelley C, Brydson M, Chauplannaz G, Oosterhuis H, Vincent A, Newsom-Davis J, Colquhoun D and Beeson D (2002) Recessive inheritance and variable penetrance of slow-channel congenital myasthenic syndromes. *Neurology* **59**:162-168.
- Croxen R, Newland C, Beeson D, Oosterhuis H, Chauplannaz G, Vincent A and Newsom-Davis J (1997) Mutations in different functional domains of the human muscle acetylcholine receptor alpha subunit in patients with the slow-channel congenital myasthenic syndrome. *Hum Mol Genet* **6**:767-774.

MOL # 44545

De Fusco M, Becchetti A, Patrignani A, Annesi G, Gambardella A, Quattrone A, Ballabio A, Wanke E and Casari G (2000) The nicotinic receptor beta 2 subunit is mutant in nocturnal frontal lobe epilepsy. *Nat Genet* **26**:275-276.

Fenster CP, Beckman ML, Parker JC, Sheffield EB, Whitworth TL, Quick MW and Lester RA (1999) Regulation of alpha4beta2 nicotinic receptor desensitization by calcium and protein kinase C. *Mol Pharmacol* **55**:432-443.

Galzi JL, Bertrand S, Corringer PJ, Changeux JP and Bertrand D (1996) Identification of calcium binding sites that regulate potentiation of a neuronal nicotinic acetylcholine receptor. *EMBO J* **15**:5824-5832.

Hamill OP, Marty A, Neher E, Sakmann B and Sigworth FJ (1981) Improved patch-clamp techniques for high-resolution current recording from cells and cell-free membrane patches. *Pflugers Arch* **391**:85-100.

Hauser WA, Annegers JF and Kurland LT (1993) Incidence of epilepsy and unprovoked seizures in Rochester, Minnesota: 1935-1984. *Epilepsia* **34**:453-468.

Heron SE, Scheffer IE, Berkovic SF, Dibbens LM and Mulley JC (2007) Channelopathies in idiopathic epilepsy. *Neurotherapeutics* **4**:295-304.

Hirose S, Iwata H, Akiyoshi H, Kobayashi K, Ito M, Wada K, Kaneko S and Mitsudome A (1999) A novel mutation of CHRNA4 responsible for autosomal dominant nocturnal frontal lobe epilepsy. *Neurology* **53**:1749-1753.

Itier V and Bertrand D (2002) Mutations of the neuronal nicotinic acetylcholine receptors and their association with ADNFLE. *Neurophysiol Clin* **32**:99-107.

Leniger T, Kananura C, Hufnagel A, Bertrand S, Bertrand D and Steinlein OK (2003) A new chrna4 mutation with low penetrance in nocturnal frontal lobe epilepsy. *Epilepsia* **44**:981-985.

Lewis TM, Sivilotti LG, Colquhoun D, Gardiner RM, Schoepfer R and Rees M (1998) Properties of human glycine receptors containing the hyperekplexia mutation alpha1(K276E), expressed in *Xenopus* oocytes. *J Physiol* **507**:25-40.

Matsushima N, Hirose S, Iwata H, Fukuma G, Yonetani M, Nagayama C, Hamanaka W, Matsunaka Y, Ito M, Kaneko S, Mitsudome A and Sugiyama H (2002) Mutation (Ser284Leu) of neuronal nicotinic acetylcholine receptor alpha4 subunit associated with frontal lobe epilepsy causes faster desensitization of the rat receptor expressed in oocytes. *Epilepsy Res* **48**:181-186.

Meisler MH, Kearney J, Ottman R and Escayg A (2001) Identification of epilepsy genes in human and mouse. *Annu Rev Genet* **35**:567-588.

Miyazawa A, Fujiyoshi Y, Stowell M and Unwin N (1999) Nicotinic acetylcholine receptor at 4.6 Å resolution: transverse tunnels in the channel wall. *J Mol Biol* **288**:765-786.

Miyazawa A, Fujiyoshi Y and Unwin N (2003) Structure and gating mechanism of the acetylcholine receptor pore. *Nature* **424**:949-955.

MOL # 44545

- Monteggia LM, Gopalakrishnan M, Touma E, Idler KB, Nash N, Arneric SP, Sullivan JP and Giordano T (1995) Cloning and transient expression of genes encoding the human alpha 4 and beta 2 neuronal nicotinic acetylcholine receptor (nAChR) subunits. *Gene* **155**:189-193.
- Moulard B, Picard F, le Hellard S, Agulhon C, Weiland S, Favre I, Bertrand S, Malafosse A and Bertrand D (2001) Ion channel variation causes epilepsies. *Brain Res Brain Res Rev* **36**:275-284.
- Mulley JC, Scheffer IE, Petrou S and Berkovic SF (2003) Channelopathies as a genetic cause of epilepsy. *Curr Opin Neurol* **16**:171-176.
- Phillips HA, Favre I, Kirkpatrick M, Zuberi SM, Goudie D, Heron SE, Scheffer IE, Sutherland GR, Berkovic SF, Bertrand D and Mulley JC (2001) CHRNA2 is the second acetylcholine receptor subunit associated with autosomal dominant nocturnal frontal lobe epilepsy. *Am J Hum Genet* **68**:225-231.
- Quick MW and Lester RA (2002) Desensitization of neuronal nicotinic receptors. *J Neurobiol* **53**:457-478.
- Rees MI, Lewis TM, Kwok JB, Mortier GR, Govaert P, Snell RG, Schofield PR and Owen MJ (2002) Hyperekplexia associated with compound heterozygote mutations in the beta-subunit of the human inhibitory glycine receptor (GLRB). *Hum Mol Genet* **11**:853-860.
- Rodrigues-Pinguet N, Jia L, Li M, Figl A, Klaassen A, Truong A, Lester HA and Cohen BN (2003) Five ADNFLE mutations reduce the Ca²⁺ dependence of the {alpha}4{beta}2 acetylcholine response. *J Physiol* **550**:11-26.
- Sands SB and Barish ME (1991) Calcium permeability of neuronal nicotinic channels in PC12 cells. *Brain Res* **560**:38-42.
- Séguéla P, Wadiche J, Dineley-Miller K, Dani JA and Patrick JW (1993) Molecular cloning, functional properties and distribution of rat brain alpha7: A nicotinic cation channel highly permeable to calcium. *J Neurosci* **13**:596-604.
- Steinlein OK (2002) Channelopathies can cause epilepsy in man. *Eur J Pain* **6**:27-34.
- Steinlein OK (2008) Human disorders caused by the disruption of the regulation of excitatory neurotransmission. *Results Probl Cell Differ* **44**:223-242.
- Steinlein OK, Magnusson A, Stoodt J, Bertrand S, Weiland S, Berkovic SF, Nakken KO, Propping P and Bertrand D (1997) An insertion mutation of the CHRNA4 gene in a family with autosomal dominant nocturnal frontal lobe epilepsy. *Hum Mol Genet* **6**:943-947.
- Steinlein OK, Mulley JC, Propping P, Wallace RH, Phillips HA, Sutherland GR, Scheffer IE and Berkovic SF (1995) A missense mutation in the neuronal nicotinic acetylcholine receptor alpha 4 subunit is associated with autosomal dominant nocturnal frontal lobe epilepsy. *Nat Genet* **11**:201-203.

MOL # 44545

MOL # 44545

Footnotes

This work was supported by the National Health and Medical Research Council of Australia to S.B. J.M and I.S., the Deutsche Forschungsgemeinschaft to O.K. (grant STE16511-1) and D.B. (grants from the Swiss National Science Foundation 3100A0-101787/2 and Deutsche Forschungsgemeinschaft Schwerpunktprogramm SPP 1226).

MOL # 44545

Figure legends

Figure 1 Sequence alignment and mutation positions.

A, C) Pedigrees of families Hn ,C and A138 with their typical chromatograms of the sequence where the mutations are located. Affected individuals are indicated by filled symbols, stars show subjects tested positive for mutations. Proband is indicated by arrows. **B, D)** nAChR genes and corresponding protein sequences with homologies (indicated by box) at amino acid positions 301 and 308 in *CHRNA2*. **E)** Left, schematic representation of the nAChR embedded in the cell plasma membrane derived from the high-resolution electron microscopic images (Miyazawa et al., 1999). Right, diagram of the putative transmembrane organization of the nAChRs based on the model proposed by Le Novère and Changeux (1999). (⊗) β 2-V287M, (*) β 2-L301V and (+) β 2-V308A indicate positions of the mutations with respect to the putative structure of the transmembrane domains.

Figure 2 Mutations increase the ACh sensitivity.

Representative ACh-evoked currents recorded in control and mutant β 2-L301V containing receptors in the heterozygous mode (**A**), β 2-V308A (**B**). Left panels, currents evoked by increasing ACh concentrations recorded in oocytes expressing mutant receptors or sibling oocytes expressing control receptors. Bars above the traces indicate the duration of the agonist application. Values on the left of each trace indicate the applied ACh concentration (in μ M). Right panels, dose-response curves recorded for controls (open circles **A**, n= 10; **B**, n= 9 and **C**, n=9) and the mutant containing receptors (filled squares **A**, n= 22; **B**, n= 10; **C**, n= 8). Data points are expressed as mean values \pm SEM. Continuous lines through the data points are the best fits according to equation (1). Values of the parameters are given in Table 1.

Figure 3 Mutations affect current amplitude and receptor sensitivity.

A) Bars correspond to the mean current values recorded in a series of oocytes. **B)** Mutations effect on the dose-response parameters. Histograms represent the ratios between control and mutants

MOL # 44545

computed as follows, column a = $a_{\text{Mutant}}/a_{\text{CT}}$, $EC_{50H} = EC_{50HCT}/EC_{50HMutant}$ and $EC_{50L} = EC_{50LCT}/EC_{50LMutant}$ (Values used for the ratio computations are presented in Table 1). CT refers to the values of the control $\alpha 4\beta 2$ nAChR whereas Mutant refers to the $\beta 2$ -L301V and $\beta 2$ -V308A respectively. Statistically significant differences are indicated by the * ($P < 0.05$).

Figure 4 Decay time course of the ACh evoked currents.

A) Average currents recorded in controls ($n=12$) and evoked by three ACh concentrations are superimposed. Values were sampled every 250 ms and represented as mean and standard errors. To improve visibility lines were drawn between data points. Continuous curves correspond to the best fit obtained with a single exponential (methods, Equation (3)) and their values are summarized in Table 2. Time zero corresponds to the beginning of the recording while exponential decay was adjusted with a time zero at the peak of ACh-evoked currents. Fraction of currents presented in **A**, **B** and **C** correspond to 25, 50 and 100% of the responses evoked by 1 mM ACh. **B), C)** Data obtained in oocytes expressing receptors with the $\beta 2$ -L301V ($n = 9$) and $\beta 2$ -V308A ($n=12$) mutations, respectively, are represented. Criteria and data treatments were the same as those described in **(A)**. **D)** Plot of the decay time constant τ as a function of the agonist concentration. In agreement with the enhanced receptor sensitivity, the ACh concentrations evoking 25% of maximal responses were shifted toward lower values for the two mutants. Note the increase of the τ values for the highest ACh test pulses in the mutants in comparison to controls. To eliminate the possible contribution of calcium activated chloride channels the same experiments were repeated in BAPTA-AM (100 μM , overnight) treated oocytes. Panels E-H were obtained in conditions similar from those shown in A-D following calcium chelation.

Figure 5 Expression of control and mutated nAChRs in mammalian cells.

A) Typical whole cell current recordings evoked by brief ACh pulses (100 μM , 400 ms) for the control, the $\beta 2$ L301V and $\beta 2$ V308A. Time constant of desensitization was determined by curve fitting with a single exponential and a constant in the form $y = -A * \exp -t/\tau + B$, where y = the current in pA, t = the time in ms, A , τ and B are constants. Cells were held at -100 mV and time constant \pm standard error of mean for each cDNA type are indicated under the corresponding

MOL # 44545

traces. **B) $\beta 2$ mutations do not modify single channel conductance.** Typical outside-out recordings from patches pulled from cells expressing the control (CT- $\alpha 4\beta 2$) and mutated ($\beta 2$ -V287M, $\beta 2$ -L301V and $\beta 2$ -V308A) nAChRs are shown in the upper traces. These traces illustrate the inward deflection observed when the channel is open (o) versus closed (c). Bars above the traces indicate the timing of ACh application. The current amplitude observed during single channel opening is not affected by the mutation (dashed line). Cumulative amplitude histograms obtained from at least three individual patches are shown in the lower panel. Continuous lines are the best fit obtained using Gaussian distributions and single channel amplitudes of -2.9 pA for $\beta 2$ V287M and $\beta 2$ L301V, -3.05 pA for $\beta 2$ V308A and -3.1 pA for controls, which respectively yield main single channel conductances of 42, 43 and 45pS. Multiple openings, such as observed for the $\beta 2$ -V287M mutant, are indicative of the activity of at least three receptors within the patch, and can be fitted with multiple Gaussians using the same conductance.

Figure 6 Sustained nicotine exposure desensitize the $\alpha 4\beta 2$ nAChR.

A) Traces presented in the left panel illustrate the typical effects of a sustained nicotine exposure on ACh-evoked currents for the control (CT- $\alpha 4\beta 2$, open circles) and ADNFLE mutants ($\beta 2$ -V287M solid diamonds, $\beta 2$ -L301V solid triangles and $\beta 2$ -V308A solid squares). Sensitivity of the cell was tested at 90 s intervals by a brief ACh test pulse (30 μ M, 3 μ M and 10 μ M respectively, 2s). These ACh concentrations roughly activate half of the receptors. Following a stabilization period, nicotine is applied in the bath and ACh responses recorded again. Note the progressive reduction of the ACh-evoked current during the sustained nicotine exposure. Same experiments were repeated for a series of nicotine concentrations allowing to examine the relationship between nicotine concentration and fraction of inhibition. **B)** Plot of the peak ACh-evoked current recorded after 12 minutes nicotine exposure, as a function of the nicotine concentration used in desensitization experiments (left panel) yielded typical concentration-inhibition curves. Lines through the data points are the best fit obtained with the Hill equation (Equation 2, see methods). **C)** The histogram illustrates the difference in nicotine IC_{50} 's of the mutants versus the control receptors. Number of cells measured for each construct is indicated in parenthesis and statistically significant differences

MOL # 44545

from the controls by the asterisk. To minimize effects caused by the activation of calcium dependent chloride currents, all data have been recorded from cells treated with the calcium-chelating agent BAPTA-AM (100 μM > 3 hours). All data have been obtained from heterozygous expression of the mutated and non-mutated alleles injected at equimolar cDNA concentrations.

Figure 7 Nicotine activation and desensitization define a window current.

Nicotine desensitization profiles for the control (CT- $\alpha 4\beta 2$), and three ADNFLE mutant receptors ($\beta 2$ -V287M, $\beta 2$ -L301V and $\beta 2$ -V308A) are presented together with the respective activation profiles (filled symbols). As in Figure 6, all data have been obtained from heterozygous expression. Bars indicate the standard error of mean. Continuous curves through the data points are the best fits obtained with Equation 2 for the desensitization and Equation 1 for the activation (see methods). Respective values obtained from these fits were: CT- $\alpha 4\beta 2$ $EC_{50H} = 1.54 \pm 0.42$ nH_H = 0.9 ± 0.01 , a = 29 % ± 3 $EC_{50L} = 10.3 \mu\text{M} \pm 0.42$ nH_L = 1.56 ± 0.07 (nb cells = 8), $\alpha 4\beta 2$ -V287M $EC_{50H} = 0.16 \pm 0.01$ nH_H = 0.9 ± 0.05 , a = 39 % ± 0.01 $EC_{50L} = 2.68 \mu\text{M} \pm 0.42$ nH_L = 1.76 ± 0.08 (nb cells = 5), $\alpha 4\beta 2$ -L301V $EC_{50H} = 1 \pm 0.18$ nH_H = 1 ± 0.02 , a = 19 % ± 0.01 $EC_{50L} = 9.75 \mu\text{M} \pm 1.28$ nH_L = 1.7 ± 0.11 (nb cells = 4), $\alpha 4\beta 2$ -V308A $EC_{50H} = 1.35 \pm 0.39$ nH_H = 0.94 ± 0.02 , a = 30 % ± 4 $EC_{50L} = 6.7 \mu\text{M} \pm 0.75$ nH_L = 1.4 ± 0.01 (nb cells = 5). Dash lines indicate the best fits obtained for the control receptor (CT- $\alpha 4\beta 2$). The grey areas indicate the window currents that are the overlap between desensitization and activation. Note the important shift in the window currents between the control and mutated receptors independently of the increased ACh sensitivity. Cells were treated with BAPTA-AM as in Figure 6.

MOL # 44545

Table 1. Acetylcholine affinity at different ADFLE receptor mutants

Receptor subtype	Mode of expression	a	EC ₅₀ H (μM)	nH1	1-a	EC ₅₀ L (μM)	nH2	n
Control (α4β2)	Homozygote	25 ± 2	5.8 ± 0.8	1.0 ± 0.05	75	63.9 ± 7.2	1.4 ± 0.05	45
β2-L301V	Homozygote	63 ± 1 *	0.9 ± 0.2 *	1.5 ± 0.14	37 *	18.8 ± 2.8 *	0.8 ± 0.02	6
	Heterozygote	56 ± 3 *	3.8 ± 1.2 *	1.3 ± 0.06	44 *	41.2 ± 6.7	0.9 ± 0.05	22
β2-V308A	Homozygote	57 ± 8 *	0.5 ± 0.1 *	1.8 ± 0.10	43 *	21.0 ± 3.8 *	1.4 ± 0.2	10
	Heterozygote	53 ± 4 *	1.6 ± 0.3 *	1.4 ± 0.09	47 *	37.4 ± 2.1	1.3 ± 0.07	13
β2-V287M	Homozygote	79 ± 2 *	0.3 ± 0.0 *	1.6 ± 0.15	21 *	2.9 ± 0.9 *	1.9 ± 0.15	7
	Heterozygote	65 ± 3 *	0.4 ± 0.1 *	1.6 ± 0.13	35 *	5.3 ± 2.3 *	1.0 ± 0.05	7

a, EC₅₀H, nH1 = percentage of receptors in the high-affinity state, half-effective concentration, and Hill coefficient; 1-a, EC₅₀L, nH2 = percentage of receptors in the low-affinity state, half-effective concentration and Hill coefficient; values are mean ± SEM; n = number of cells tested; * = significantly different from the corresponding control values, P = <0.05.

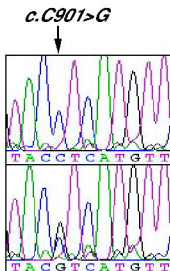
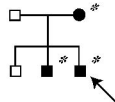
MOL # 44545

Table 2. Response decay time constants at three ACh concentrations

Receptor subtype	ACh (μ M)	τ (s)	P value	n	ACh (μ M)	τ (s)	P value	n
CT- α 4 β 2	10.6 \pm 3.2	1.75 \pm 0.25		12	10.6 \pm 3.2	7.7 \pm 1.4		3
	40.5 \pm 8.8	1.21 \pm 0.19		12	40.5 \pm 8.8	6.8 \pm 1.0		3
	767 \pm 62	1.33 \pm 0.16		12	767 \pm 62	6.5 \pm 0.7		3
α 4 β 2-L301V	1.6 \pm 0.9	1.13 \pm 0.11	0.005	9	6.7 \pm 1.3	7.7 \pm 0.9	1.000	3
	6.8 \pm 4.7	0.84 \pm 0.07	0.058	9	42.7 \pm 10.6	7.3 \pm 1.2	0.767	3
	1000 \pm 0	6.30 \pm 1.09	0.003	9	341 \pm 85	14.8 \pm 5.1	0.247	3
α 4 β 2-V308A	1.3 \pm 0.4	1.25 \pm 0.13	0.098	12	6.6 \pm 1.3	8.3 \pm 1.2	0.742	3
	8.4 \pm 2.3	1.09 \pm 0.11	0.706	12	26.7 \pm 5.3	11.3 \pm 2.8	0.025	3
	900 \pm 40	5.35 \pm 1.14	0.0001	12	426 \pm 85	6.5 \pm 1.5	1.000	3

The ACh concentrations are the mean of concentrations used for each cell tested to evoke 25, 50, 100% of the maximal response; values are mean \pm SEM; n = number of cells tested; for BAPTA condition cells were incubated in BAPTA-AM (100 μ M) overnight before measurements.

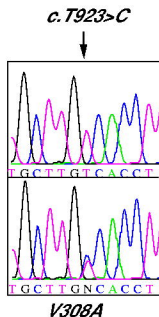
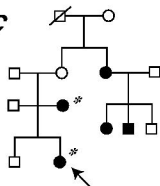
A Family Hn



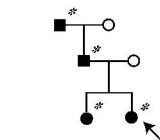
Family C

L301V

C



Family A138



B

Mutated allele		301									
Human	CHRN2	L	V	G	K	Y	L	M	F	T	M
	CHRN1	I	I	I
	CHRN3	.	I	.	E	.	.	L	.	I	.
	CHRN4	.	I
	CHRNA2	.	.	I	.	E	.	.	L	.	.
	CHRNA3	.	I	.	E	.	.	L	.	.	.
	CHRNA4	.	I	.	E	.	.	L	.	.	.
	CHRNA5	.	.	I	.	E	.	.	V	.	.
	CHRNA6	.	.	.	E	.	.	L	.	.	.
	CHRNA7	.	I	A	Q	.	F	A	S	.	.
	CHRNA9	.	I	.	.	.	Y	I	A	.	.
	CHRNA10	.	I	.	.	.	Y	.	A	.	.

D

Mutated allele		308									
Human	CHRN2	Y	L	M	F	T	M	I	L	V	S
Chick	CHRN2
Rat	CHRN2
Fish	CHRN2
Dros.m	CHRN2	.	L
Bovine	CHRN2	V	.	F
Human	CHRN4
Chick	CHRN4
Human	CHRNA4	F	.	F
Human	CHRNA3	.	L	F	.	F
Human	CHRNA5	.	V	F	.	F
Human	CHRN1	V	.	F

E

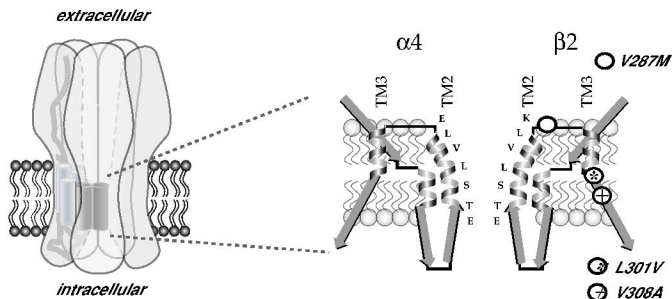


Figure 2

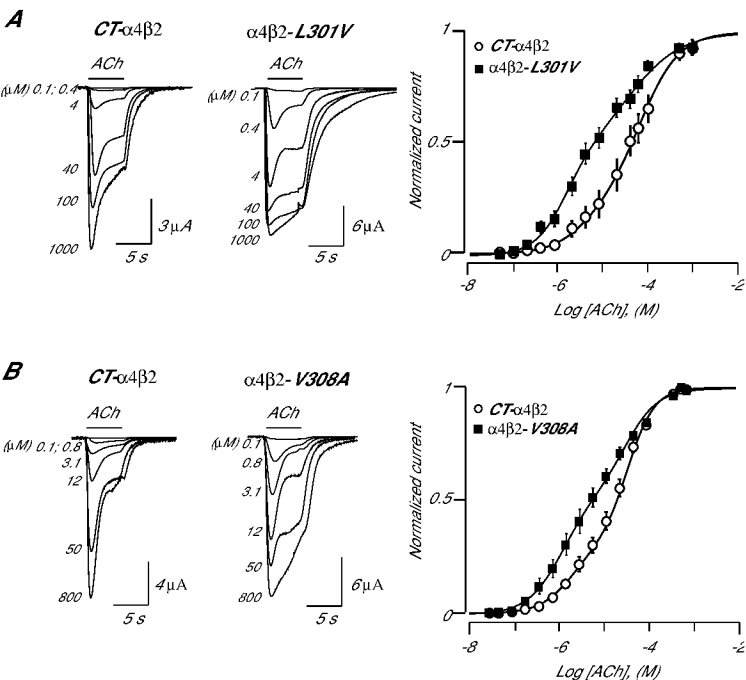
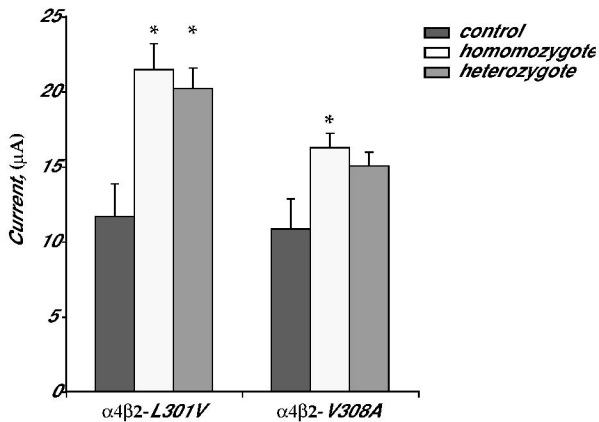
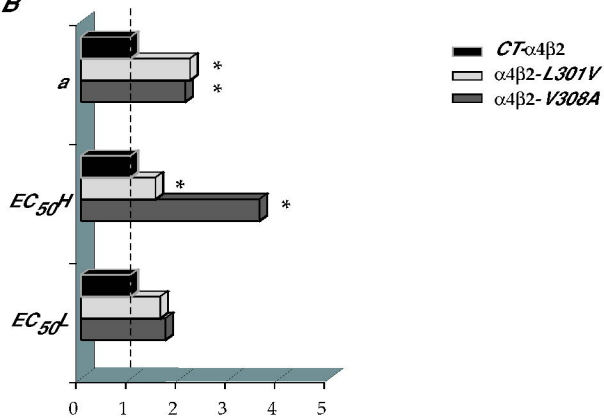


Figure 3

A



B



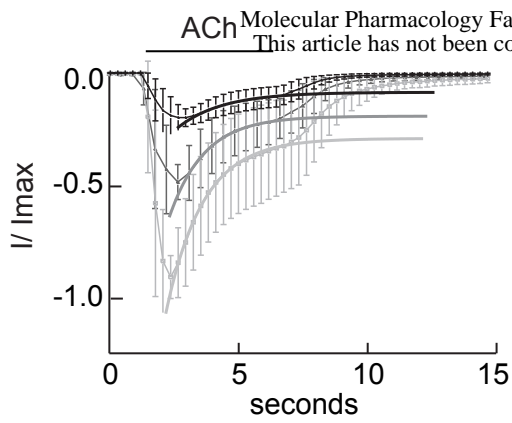
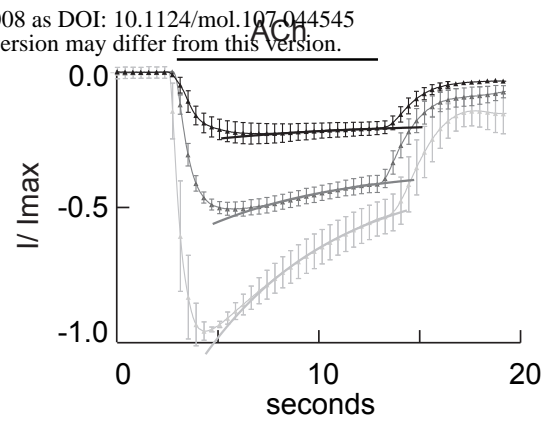
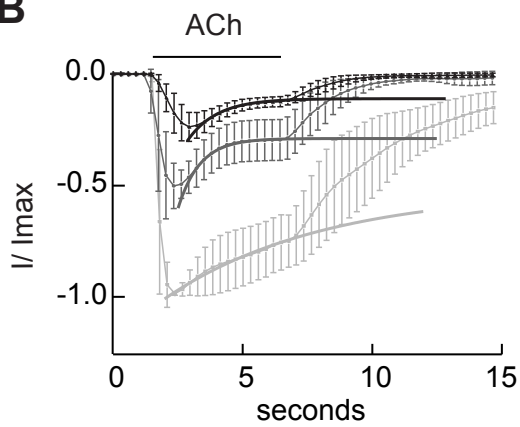
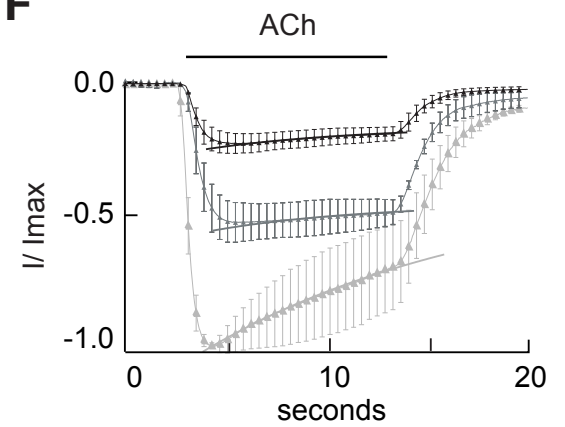
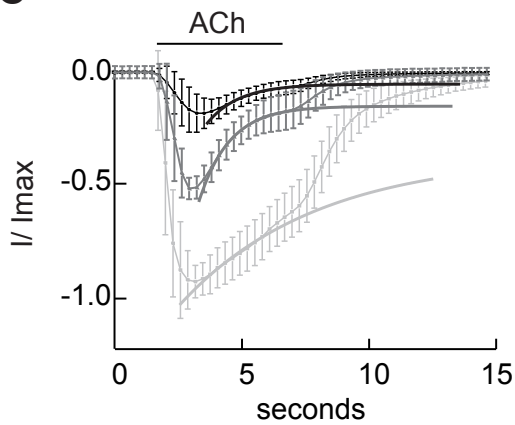
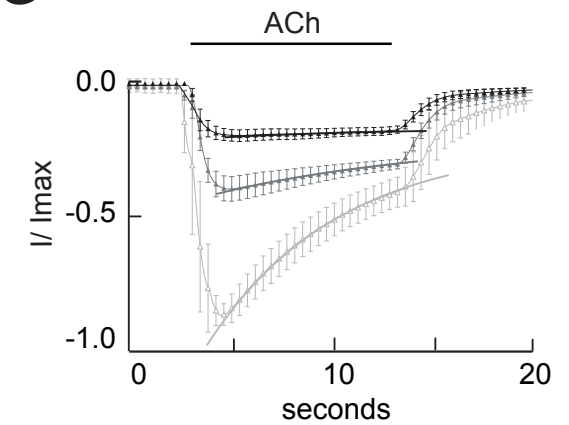
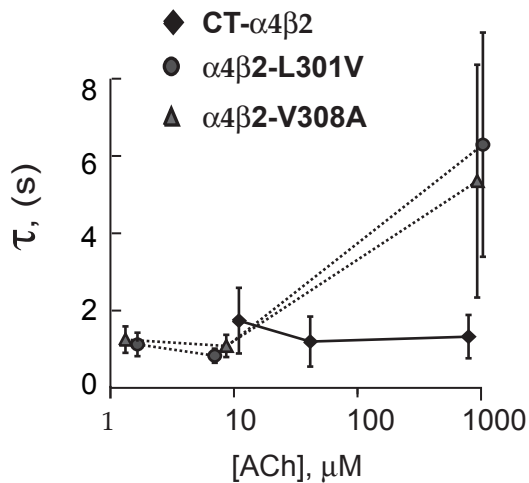
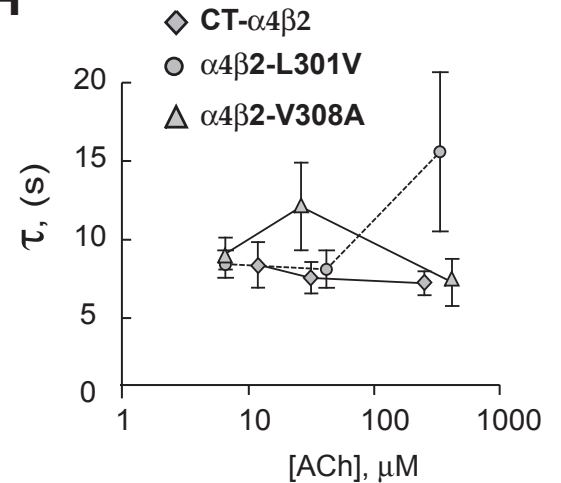
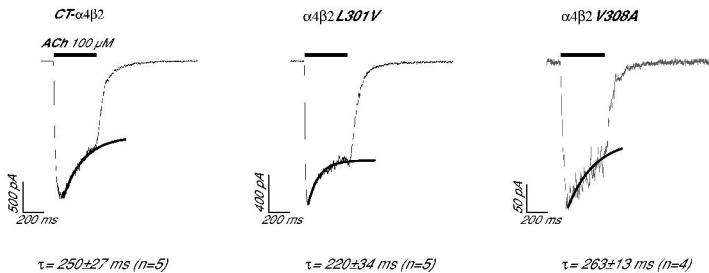
No-BAPTA**A****BAPTA****E****B****F****C****G****D****H**

Figure 5

A



B

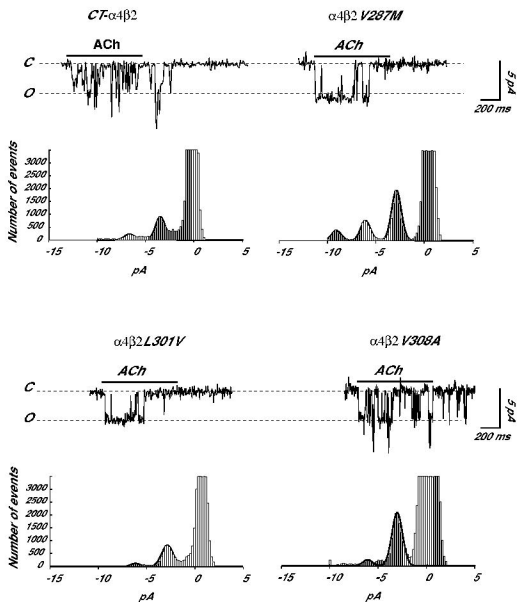
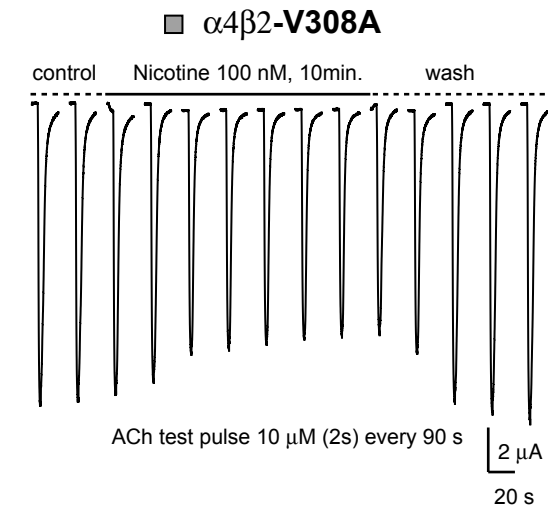
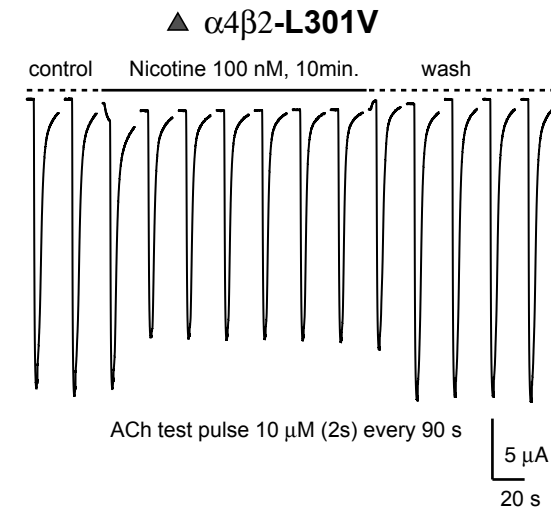
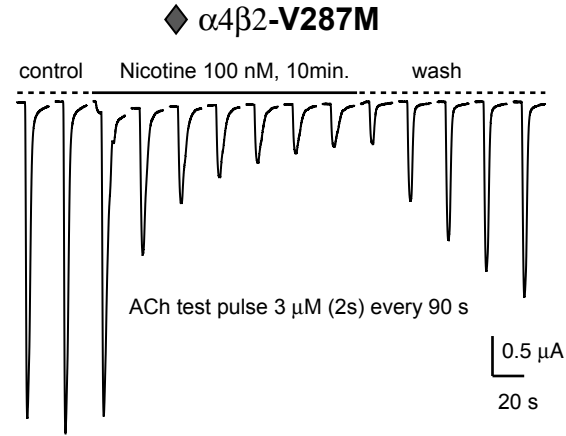
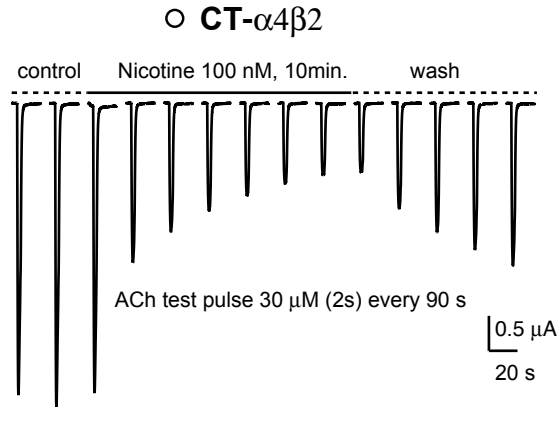
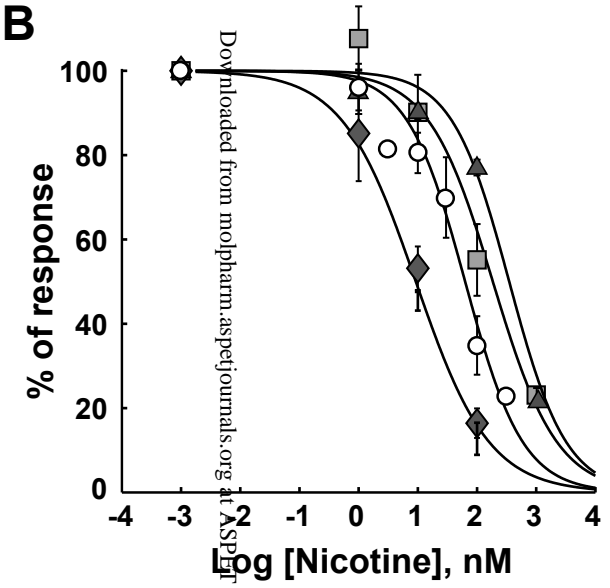


Figure 6

A



B



C

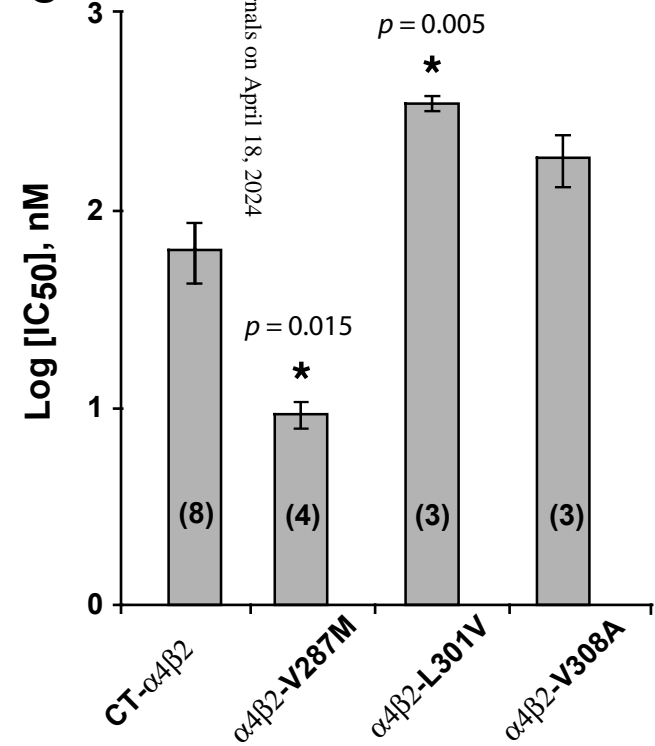


Figure 7

